# Exploiting Typical Clinical Imaging Constraints for 3D Outer Bone Surface Segmentation

Chris Mack, Vishali Mogallapu, Andrew Willis, Thomas P. Weldon
*UNC Charlotte, Department of Electrical and Computer Engineering*
*Charlotte, NC, USA*
*contact email : tpweldon@uncc.edu*

## Abstract

*We present a method for extracting outer bone surfaces from a 3D CT (computer tomography) image sequence using a novel segmentation scheme on each image. A 3D mesh of the bone surface is then generated using the marching cubes algorithm. The new segmentation algorithm makes use of several imaging constraints which greatly simplify the problem including : (i) the cross-sectional size of a bone is approximately known and (ii) the geometric shape of a cross-section is approximately known. In clinical practice using commerical CT scanners, these quantities are typically known and serve to greatly simplify the segmentation problem. By segmenting the image data, the algorithm is capable of uniquely extracting the bone outer surface in contrast to other methods which often include extra surfaces or surfaces with holes. This paper presents the segmentation method and shows results for extracting tibia bone outer surfaces.*

## 1 Introduction

Advances in medical imaging have made 3D images an important tool for planning, diagnosis, and treatment of medical problems. Yet, these images often include information that is irrelevant to these tasks. Tools capable of extracting bone surfaces from 3D medical data are then important in contexts which require detailed knowledge of bone outer surfaces and their relative orientations. Two such situations are orthopaedic surgery planning and kinematic analysis of articulating limb joints.

The importance of this problem has warranted numerous research papers on the subject. One such paper [1] uses Color Structure Codes (CSC) to segment bones from CT images. Another paper by Sonka et. al. [2] uses a topologically constrained version of the Sethian's now pervasive level set method [3]. While these methods produce effective results, an algorithm capable of segmenting all bone structures remains to be defined. The methods of this paper suggest an alternative approach. Rather than treating segmentation as a completely unconstrained shape estimation problem, we exploit both the typical relative geometry between commercial imaging systems and the standard orientation of human subjects when imaged within these systems. This assumed relative geometry between the sensor and the patient provides powerful constraints that aid greatly in the segmentation problem. For typical commerical CT scanners, the imaged patients are oriented in the device as shown in figure 1.

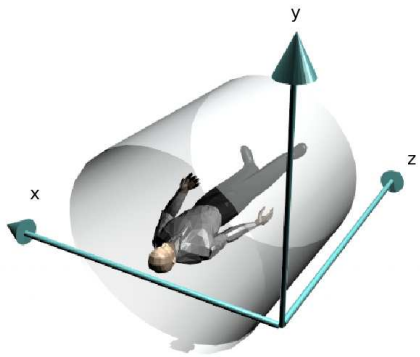


Figure 1: The coordinate system of the CT scan 3D data. Each image provides measurements of a 3D image for a specific $z$ value. For the slice at position $z = z_0$, the measured CT image provides discrete samples from an unknown continuous mathematical function $I(x, y, z_0)$.

In the proposed method, segmented images serve as input to a polygonization routine which provides a 3D mesh description of the outer bone surface. The de-facto standard for this step has become the "Marching Cubes" method first outlined by Lorensen and Cline in [4] with numerous extensions and variants as discussed in [5, 6, 7].

The problem is complicated by variations in bone density. Figure 2 shows a typical cross-sectional slice of a human leg when imaged within the standard coordinate system speci-

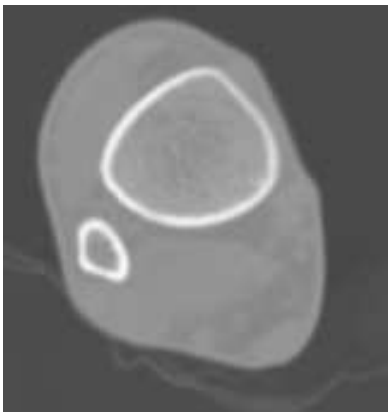

Figure 2: A typical CT image showing a mid-shaft cross-sectional slice of the tibia (center) and fibula bones (bottom left).

fied in fig. 1. The outer surface of the tibia and fibula appear as roughly circular curves in the image with high intensity values. The measured CT intensities reflect the amount of x-ray radiation absorbed by each volume of imaged tissue. Since the outer bone surface has higher density than any of the surrounding tissue, intensities at these locations are significantly higher (Fig. 2). Yet, for bones within human limbs, the outer surface bone density varies over the extent of the bone. Specifically, the mid-shaft densities are much higher than those at bone extrema. This can introduce difficulties in correctly determining the location of the outer bone surface, especially at bone extrema. For surface estimation algorithms, this leads to good surface estimates in mid-shaft areas of the bone but poor surface estimates in extremal regions, e.g., for the tibia the estimate is worse as the bone gets closer to the foot (Fig. 3). The variation in density is illustrated as the lower extremety dissappears when the threshold of 215 in Fig. 3(a) is increased to 247 in Fig. 3(b).

The marching cubes method also captures both the inside and outside surface of the bone cortical tissue whereas only the outside surface is typically of interest (Fig. 5). Therefore, the proposed method also removes the inner surface of bone structure.

## 2 Approach

A contribution of this paper is to automatically eliminate spurious surfaces such as the inside cortical surface by exploiting three constraints : (i) human limbs are typically oriented parallel to the coordinate system $z$-axis, (ii) cross-sections of bones within these limbs are typically well-approximated by quadric surfaces such as ellipses, and (iii) the size of human limb-bones do not exhibit large amounts of variation.

These constraints serve to form our segmentation approach which consists of three steps :

(a) (b)

Figure 3: Two outputs from standard marching cube segmentations. (a) shows a bone segmentation generated by thresholding the CT image data at an 8-bit grey value of 215. (b) Shows a bone segmentation obtained by extracting levelset 247 from the 3D CT data.

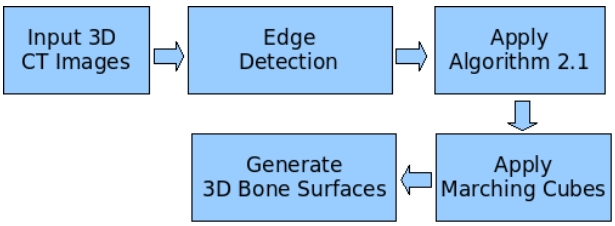


Figure 4: Steps of the algorithm.

1. Compute the 2-dimensional gradient-magnitude images by applying equation (1) which follows the edge computation technique proposed by Canny in [8].

$$\|\bigtriangledown I(x, y, z_0)\| = \sqrt{\frac{\partial I}{\partial x}^2 + \frac{\partial I}{\partial y}^2} \qquad (1)$$

2. Solve a 1-dimensional segmentation problem as detailed in §2.1,

3. Polygonize the bone outer surface using the standard marching cube algorithm by implementing, in Java, the code made available by Bourke and Ward [9].

Since steps 1 and 3 of this process apply well-known algorithms, we first describe the details of the segmentation problem in §2.1 and then briefly describe the isosurface extraction procedure in §2.2.

Figure 5: 3D model showing that inner bone surfaces were extracted using marching cubes.

## 2.1 Bone Surface Segmentation as 1D Peak Detection

As mentioned in §2, the cross-sectional shape of the bone tends to remain constant over slices along the z-axis and may be well-approximated by a 2D quadric surface such as an ellipse within slices. By viewing each image slice row as a 1-dimensional signal, edges due to outer bone surfaces generate peaks within this signal. We may then view the segmentation problem as a peak detection problem where we seek to find the constellation of peaks that are most likely to delineate the outer surfaces of a bone within the CT image data.

Given that outer bone surface cross-sections within each image are well-approximated by a quadric curve, we may use results from algebraic geometry to assist in solving our 1-dimensional peak detection problem within the image row. Specifically we may use Bézout's theorem which states :

> *"Two algebraic curves of degrees $m$ and $n$ intersect in (at most) $mn$ points and cannot meet in more than $mn$ points unless they have a component in common (i.e., the equations defining them have a common factor; [10])."* (quoted from [11])

For a given slice, $z_0$, we now process each image row and consider the row to be a horizontal line $y = y_0$. Peaks in the intensity function for that row $I(x, y_0, z_0)$ then correspond to intersections of this line with cortical surfaces within the image. Bézout's theorem then dictates that each cortical bone surface will generate at most 2 peaks in the intensity function. As each bone has both an inner and outer cortical surface, up to four peaks may be generated in the intensity function by a single bone in the CT image. Imaged peaks must also be spatially local to one another to have been generated by a human bone. Auxillary information included in generated DICOM images include the $(x, y, z)$ dimension of the CT image voxels. Using this information, we dictate that the outer cortical surface of a given bone must be $<5$ cm. in length (note we are typically dealing with bone cross-sectional slices). Given these assumptions, there exist several other potential methods for isolating the boundary of the outer bone surface. Examples include the convex hull algorithm (see [12] for details) and various line-clipping algorithms (see [13] for several such algorithms). These methods suffer from the same uncertainties present in any segmentation situation, i.e., where the true boundary is unknown. The proposed method has performance benefits due to the assumption that unknown boundary curves in each image are quadric.

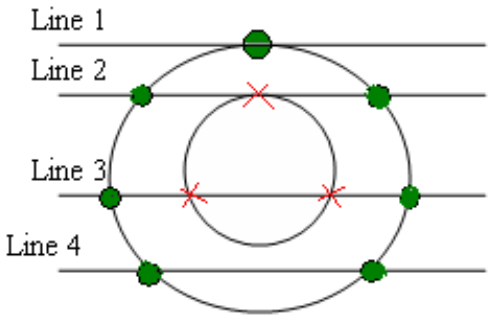


Figure 6: Different cases of a line intersecting a donut shaped curve representing the cross-section of a human bone.

Four possible cases exist as shown in Fig. 6. If only one peak is detected and no peaks are found within a 5cm. interval, then the line corresponding to the row of interest is tangent to the outer bone cortical surface (shown as *Line 1* in Fig. 6). If only two peaks are detected within a 5cm. interval, then the line corresponding to the row of interest passes through *only* cortical tissue between the detected peaks (shown as *Line 4* in Fig. 6). If only three peaks are detected within a 5cm. interval, then the line corresponding to the row of interest passes through cortical tissue and is tangent to the inner cortical surface (shown as *Line 2* in Fig. 6). If only four peaks are detected within a 5cm. interval, then the line corresponding to the row of interest passes through both the inner and outer cortical surfaces (case 1 shown as *Line 3* in Fig. 6).

Having detected peaks of the intensity function for each bone, we then proceed to set all pixels inside of an outer bone surface to 0 and outside 1, i.e., we generate a binary image as shown in Fig. 7(d).

## 2.2 Generating a 3D Mesh

The marching cubes algorithm works on any function which may be expressed as an implicit surface (2).

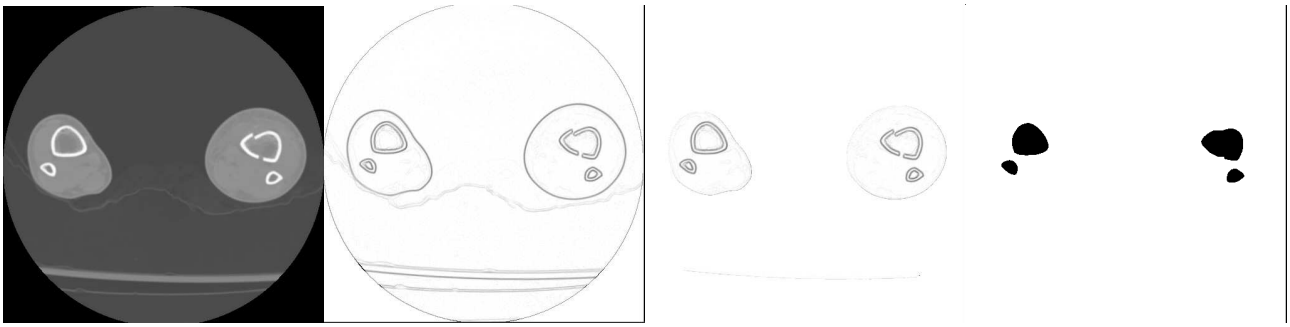

(a) (b) (c) (d)

Figure 7: Results for each step of the segmentation algorithm given a cross-sectional CT image of a patient's legs : (a) the raw image data, note that 4 bones are present including the left and right tibia and fibula, (b) the edge magnitude image, (c) the thresholded edge image, and (d) the segmented image. Note that the algorithm is still able to capture the shape of the bone outer surface despite the presence of a fracture passing through the right hand side tibia.

$$I(x, y, z) = 0 \tag{2}$$

The roots of this equation, i.e., where $I(x, y, z) = 0$, defines a continuous 3D surface. Measured $(x, y, z)$ pixel intensities, denoted as $\rho$, provide discrete samples from $I$ that lie on a uniformly spaced grid, e.g., for the point $(x_0, y_0, z_0)$ the isosurface will assume the value of the intensity : $I(x_0, y_0, z_0) = \rho$. Different isosurfaces within the 3D CT image may be extracted by shifting the equation by a constant $k$ as shown in equation (3). The isosurface generated for a given value of $k$ is also referred to as the $k^{th}$ image level set [3].

$$I(x, y, z) - k = 0 \tag{3}$$

The marching cubes algorithm solves equation (3) for a given value of $k$ to provide an estimate of the unknown 3D surface.

# 3 Results

DICOM images were obtained from the lower limb and include the left and right tibia, fibula, and bones from the ankle and foot. These images have resolution 512x512 pixels and each pixel is square with each side have physical dimension $0.5mm$. Our resulting maximum bone thickness is then 100 pixels $(5cm.)$.

We present results for one of approximately 300 CT images included in the scan. The raw data for this slice is provided as Fig. 7(a). The raw edge magnitude image is shown in Fig. 7(b). This image is subsequently thresholded to remove spurious small-magnitude edges due to non-cortical structures within the image generating the image as shown in Fig. 7(c). We then apply the segmentation algorithm described in section §2 generating the binary image shown in Fig. 7(d).

Figure 8: Incorrect segmentation results. These typically occur in regions where the threshold for extracting cortical bone surface edges is set too high. For the experimental set of 300 images similar such errors were observed in approximately 10% of the total image set.

Towards the extrema of the tibia a fibula the segmentation experiences some errors. Figure 8 shows one such error. This error exhibits two sources of possible failure for the proposed approach that remain to be addressed : (i) multiple bones may lie in close vicinity and on a common image row and (ii) thresholding the edge image may reject valid outer bone surface boundary locations.

Using the segmentation results for all of the recorded CT images, the outer bone surface was extracted by applying the marching cube algorithm on the isosurface : $I(x, y, z) - 0.5 = 0$, i.e., levelset 0.5. The final result of the marching cubes algorithm for the segmented images is shown in Fig. 9(a). One can see here that the algorithm is able to reliably extract the unique outer bone surface along the bone

mid-shaft but suffers from errors as we approach the extrema (shown at the bottom of Fig. 9(a)).

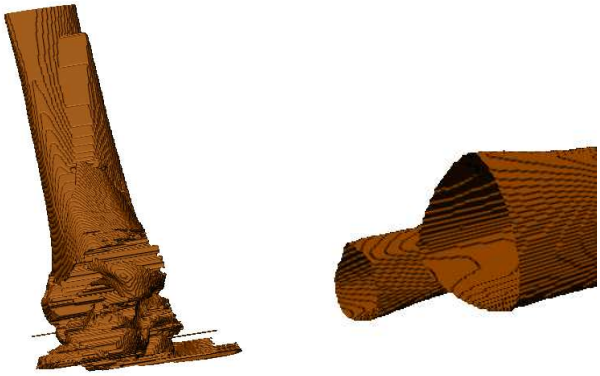

(a) (b)

Figure 9: Output of marching cubes algorithm on segmented CT data : (a) shows a profile view and (b) shows the inside of the extracted 3D surface demonstrating that *only* the bone outer surface has been extracted.

# 4 Conclusion

A novel approach to segmenting bone outer surfaces was proposed. The approach exploits three constraints that arise from an assumed relative geometry for the patient and the sensor and an assumed size for human bones : (i) human limbs are typically oriented parallel to the coordinate system $z$-axis, (ii) cross-sections of bones within these limbs are typically well-approximated by quadric surfaces such as ellipses, and (iii) the size of human limb-bones do not exhibit large amounts of variation. While the proposed segmentation approach is not capable of extracting perfectly the entire 3D outer bone surface, it does solve several important problems. These include : (1) detection of *only* the outer bone surface (see Fig. 9(b)) rather than the inner and outer interfaces of the cortical tissue (see Fig. 5) and (2) dealing with difficult situations where the bone surface has fractured as shown in Fig. 7(d).

# 5 Acknowledgements

The authors of this paper would like to acknowledge the contribution of Dr. Thomas Brown and Dr. Donald Anderson from the University of Iowa Orthopaedic Biomechanics Laboratory in providing the CT scan data used in this project.

# References

[1] P. Sturm and L. P. H. Wang, "A csc based classification method for ct bone images," in *Third International Symposium on 3D Data Processing, Visualization and Transmission*, University of North Carolina, Chapel Hill, USA, June 2006.

[2] K. Li, S. Millington, X. Wu, D. Z. Chen, and M. Sonka, "Simultaneous segmentation of multiple closed surfaces using optimal graph searching," in *Information Processing in Medical Imaging, 19th International Conference, IPMI 2005*, pp. 406–417, July 2005.

[3] J. Sethian, *Level Set Methods and Fast Marching Methods Evolving Interfaces in Computational Geometry, Fluid Mechanics, Computer Vision, and Materials Science*. Cambridge University Press, 1999.

[4] W. Lorensen and H. Cline, "Marching cubes: A high resolution 3d surface construction algorithm," in *Proceedings of the 14th annual conference on Computer graphics and interactive techniques*, pp. 163–169, August 1987.

[5] C. Bajaj, J. Blinn, J. Bloomenthal, Marie-Paule, Cani-Gascuel, A. Rockwood, B. Wyvill, and G. Wyvill, *Introduction to Implicit Surfaces*. Morgan Kaufmann, 1997.

[6] J. Bloomenthal *Computer-Aided Geometric Design*, vol. 5, pp. 341–355, November 1988.

[7] P. Ning and J. Bloomenthal, "An evaluation of implicit surface tilers," *IEEE Computer Graphics and Applications*, vol. 13, no. 6, pp. 33–41, 1993.

[8] J. Canny, "A computational approach to edge detection," *IEEE Transactions on Pattern Analysis and Machine Intelligence*, vol. 8, Nov 1986.

[9] P. Bourke, "Polygonising a scalar field," May 2004. `http://local.wasp.uwa.edu.au/~pburke/geometry/polygonise`.

[10] J. L. Coolidge, *A treatise on Algebraic Plane Curves*, p. 10. Dover, 1959.

[11] E. W. Weisstein, "Bézout's theorem." A Wolfram Web Resource. `http://mathworld.wolfram.com/BezoutsTheorem.html`.

[12] F. Preparata and S. Hong, "Convex hulls of finite sets of points in two and three dimensions," *Communications of the ACM*, vol. 20, pp. 87–93, Feb 1977.

[13] J. Blinn, "A trip down the graphics pipeline: Line clipping," *IEEE Computer Graphics and Applications*, vol. 11, pp. 98–105, Jan 1991.